

Infrared emission from Ge metal-insulator-semiconductor tunneling diodes

M. H. Liao

Department of Electrical Engineering, National Taiwan University, Taipei, Taiwan 106, Republic of China
and Graduate Institute of Electro-Optical Engineering, National Taiwan University, Taipei, Taiwan
106, Republic of China

T.-H. Cheng

Department of Electrical Engineering, National Taiwan University, Taipei, Taiwan 106, Republic of China
and Graduate Institute of Electronics Engineering, National Taiwan University, Taipei, Taiwan 106,
Republic of China

C. W. Liu^{a)}

Department of Electrical Engineering, National Taiwan University, Taipei, Taiwan 106, Republic of China;
Graduate Institute of Electro-Optical Engineering, National Taiwan University, Taipei, Taiwan 106,
Republic of China; and Graduate Institute of Electronics Engineering, National Taiwan University, Taipei,
Taiwan 106, Republic of China

(Received 22 August 2006; accepted 15 November 2006; published online 28 December 2006)

The Ge light-emitting diode with $\sim 1.8 \mu\text{m}$ strong infrared emission is demonstrated using a metal-insulator-semiconductor tunneling structure. The intensity of a Ge device is one order of magnitude stronger than a similar Si device. At the positive gate bias, the holes in the Al gate electrode tunnel to the *n*-type Ge through the ultrathin oxide and recombine radiatively with electrons. An electron-hole-plasma model can be used to fit all the emission spectra from room temperature down to 65 K. From the measurement temperature range, the extracted band gap is $\sim 40 \text{ meV}$ lower than the reported band gap data, and the linewidth drops from 70 to 25 meV. The longitudinal acoustic phonon ($\sim 28 \text{ meV}$) and/or the band gap renormalization at high carrier density are proposed to be responsible for the reduction of photon energy. The band gap reduction on the mechanically strained *n*-type Ge and Si is also investigated experimentally and theoretically. © 2006 American Institute of Physics. [DOI: 10.1063/1.2420783]

Much effort has been devoted in seeking the possibilities of light emission using indirect band gap materials¹⁻⁴ for both scientific interest and optoelectronic applications. The $1.1 \mu\text{m}$ infrared emission from Si using the metal-insulator-semiconductor (MIS) tunneling structure was demonstrated in the past.⁵ By the Ge incorporation, the emission wavelength can be further tuned. The infrared emissions of ~ 1.3 , ~ 1.5 ,⁶ and $\sim 2 \mu\text{m}$ ⁷ wavelengths from $\text{Si}_{0.8}\text{Ge}_{0.2}$ quantum well, $\text{Si}_{0.45}\text{Ge}_{0.55}$ quantum dot, and Si/SiGe heterojunction, respectively, were also reported using a similar MIS tunneling structure. Due to the high carrier mobility, strong photon absorption,⁸ and possible integration with Si, the light emission from Ge is of great interest for scientific research and practical applications. In this letter, the $1.8 \mu\text{m}$ infrared emission from Ge MIS tunneling diode with the effects of temperature and strain is investigated. As compared with the similar Si device, the infrared emission of Ge device is much stronger (approximately ten times higher). The strain effect on Ge band gap reduction is less severe than that of Si and is consistent with the theoretical calculation.

The 2 nm oxide used in the MIS tunneling diode is grown by liquid phase deposition (LPD) at 50°C on *n*-type Ge (100) wafer.⁹ The resistivity of the 100 mm Ge wafer is in the range of $0.04\text{--}0.4 \Omega \text{ cm}$. Before oxide deposition, the sample was cleaned by a HF dip. The thickness is measured by an ellipsometer. The MIS tunneling diode has Al gate electrodes with the circular area defined by the shadow mask.

The other Al contact is on the back of the wafer. The experimental setup for measuring the electroluminescence (EL) spectra and Raman spectra, and the mechanism to apply external mechanical strain are similar to the methods used in Refs. 10 and 11.

Figure 1 shows the typical *I-V* curve of a Ge MIS tunneling diode. When the Al gate is at negative gate bias, the current is mainly controlled by the thermally generated holes.¹² For the positive bias, the holes in the Al gate electrode tunnel into the Ge, besides the electron tunneling from the Ge to the Al gate electrode. As a result, a significant tunneling current was observed at the positive gate bias. Meanwhile, the positive gate bias also attracts electrons in the Ge/oxide interface to form an accumulation layer. The momentum spread due to the localized electrons in the accumulation layer, phonons, and the Ge/oxide interface rough-

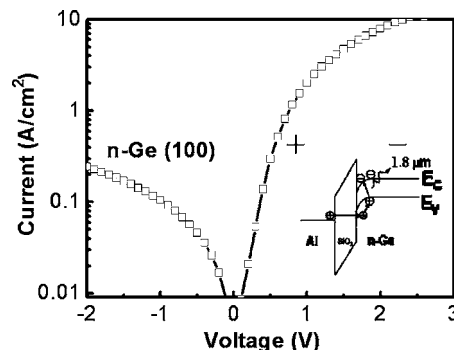


FIG. 1. *I-V* curve of a metal-insulator *n*-type Ge tunneling diode. The inset shows the schematic band diagram at the accumulation positive bias.

^{a)} Author to whom corresponding should be addressed; electronic mail: chee@cc.ee.ntu.tw

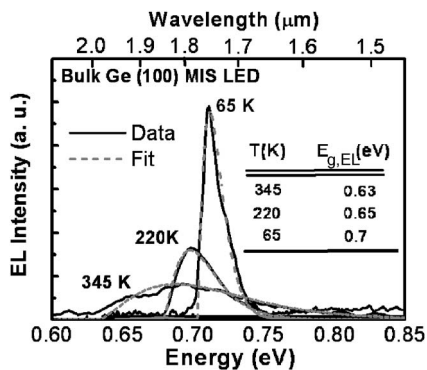


FIG. 2. Measured electroluminescence spectra of a bulk Ge (100) metal-insulator-semiconductor light-emitting diode at different temperatures. The fitting parameters such as temperature and the band gap of EL spectra are also listed for reference.

ness can provide the necessary momentum during the electron-hole radiative recombination.⁵ The luminescence was collected when the tunneling holes from Al gate electrode to Ge radiatively recombine with the electrons in the accumulation region of Ge. The band diagram of the Ge MIS light emitting diode (LED) at the positive gate bias is shown as the inset of Fig. 1 for reference. For the MIS tunneling diode with a positive gate bias, intensive infrared (Fig. 2) is emitted with a peak around $1.8 \mu\text{m}$ (0.7 eV). In order to compare the external quantum efficiency between Ge and Si MIS LEDs, two kinds of MIS tunneling diodes were fabricated by the same process, gate electrode, and LPD oxide thickness ($\sim 2 \text{ nm}$) which is controlled by the deposition time. The optical power from Si MIS LED and Ge MIS LED can be detected by two different commercial InGaAs p-i-n diodes. The spectral range of InGaAs detectors covers from 0.95 to $1.6 \mu\text{m}$ (with the responsivity of 0.65 A/W at $1.1 \mu\text{m}$) and from 1.2 to $2 \mu\text{m}$ (with the responsivity of 1.1 A/W at $1.8 \mu\text{m}$) for Si and Ge MIS LED measurements, respectively. The resulting current was read by Keithley 485 picoammeter. Under the injection current of 100 mA, the external quantum efficiency for $\sim 1.8 \mu\text{m}$ light emission from the Ge MIS LED is observed as $\sim 5 \times 10^{-5}$ at room temperature, about one order of magnitude higher than Si MIS LED at the same measurement condition. It may be due to the higher radiative recombination coefficient of Ge ($6.4 \times 10^{-14} \text{ cm}^3 \text{ s}^{-1}$ for Ge and $1.1 \times 10^{-14} \text{ cm}^3 \text{ s}^{-1}$ for Si) (Ref. 13) and the slightly smaller wave vector k needed to conserve momentum in Ge. However, the clear origin is still unknown and worthy of investigation. Note that in our quantum efficiency measurement, we cannot collect all the light from the device, and only the scattered light from the periphery of the gate area was detected. Therefore, the number presented here is a lower bound of the true quantum efficiency. The feature of the emission line shape is the asymmetrical broadening, where the high energy part is broader than the low-energy part. This is very similar to the line shape of the electron-hole-plasma (EHP) recombination in Si.⁵ To confirm this observation, the line shape of EL spectra (Fig. 2) is fitted by the EHP recombination model using the following expression:

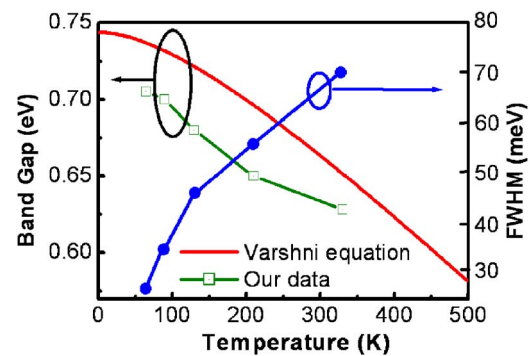


FIG. 3. Extracted band gap and linewidth at different temperatures.

$$I(h\nu) = I_0 \int_0^{h\nu - E_{g,EL}} dE D_e(E) D_h(h\nu - E_{g,EL} - E) f_e(E, F_e, T) f_h(h\nu - E_{g,EL} - E, F_h, T),$$

where D_e and D_h are the densities of states of electrons and holes, respectively, F_e and F_h are the respective quasi-Fermi energies, $h\nu$ is the energy of photon emitted, T is the measurement temperature, $E_{g,EL}$ is the band gap of Ge obtained by the EL measurement, and f are the Fermi-Dirac distribution. The fitting parameters used in this work are also listed in Fig. 2. The carrier density estimated from the quasi-Fermi energy at 65 K is about $8 \times 10^{17} \text{ cm}^{-3}$. According to the Mott transition, excitons will dissociate into electron-hole plasma at a high carrier density. The extracted band gaps from the EL spectra from Ge MIS tunneling diode are $\sim 40 \text{ meV}$ lower than the Ge band gap obtained from Varshni's equation¹⁴ for the measurement temperatures (Fig. 3), while the photon energy reduction in Si MIS tunneling diode is observed to be $\sim 80 \text{ meV}$.¹⁵ The phonon replicas can be involved in the momentum conservation of the radiative recombination and should be responsible for the photon energy reduction. In Ge, the longitudinal acoustic (LA) phonons ($\sim 28 \text{ meV}$) are strongest and prominent, while the transverse optical phonons ($\sim 58 \text{ meV}$) are favored in Si.¹⁶ On the other hand, the high carrier concentration of $\sim 8 \times 10^{17} \text{ cm}^{-3}$ causes further energy reduction of $\sim 7 \text{ meV}$ for Ge devices, based on the band gap renormalization model calculation.¹⁷ The rest of band gap lowering ($\sim 5 \text{ meV}$) maybe due to the surface bending¹⁵ or extraction errors. The band gap renormalization of Ge is less serve than that of Si.¹⁷⁻¹⁹ The linewidth (full width at half maximum) of the EL spectra decreases from 70 to 25 meV when the temperature decreases from room temperature to 65 K (Fig. 3). The carrier filling closer to the conduction-band and valence-band edges at lower temperature is responsible for the decrease in linewidth.

Figure 4 shows the EL spectra at 65 K from the unstrained and strained Ge MIS LEDs. The magnitude of strain is measured by Raman spectroscopy. Raman spectra were excited by an Ar laser (wavelength of 514 nm) and the Raman shifts of 0.91 and 1.32 cm^{-1} under uniaxial and biaxial tensile strains, respectively, were extracted from the curve fitting using a Lorentzian profile.¹¹ Using the Raman shift of the Ge-Ge phonon peak and phenomenological potentials, the strains in Ge are estimated to be 0.32% for biaxial strain and 0.45% for uniaxial strain,¹¹ respectively. The redshift of the EL spectra under the external tensile strain was observed in Ge MIS LED, similar to the Si MIS LED.¹⁰ The peak of

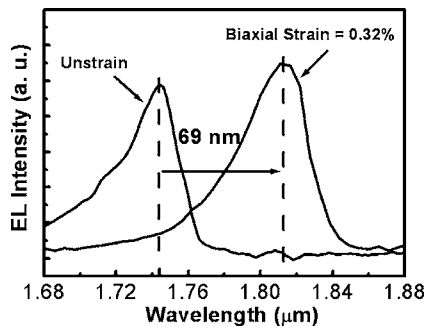


FIG. 4. Electroluminescence spectra of the Ge metal-insulator-semiconductor light-emitting diode under 0.32% biaxial tensile strain at 65 K.

the light emission spectra at the temperature of 65 K is reduced by 30 meV (69 nm) under the 0.32% external biaxial tensile strain. Band gap reduction as a function of external strain for Ge and Si is shown in Fig. 5 with the theoretical curves. Both Ge and Si band gaps are reduced under the tensile strain. Using the deformation potential parameter in Ref. 19, with the formula in Ref. 20, the theoretical values of band gap reduction (ΔE_g) of Ge (Si) due to external strain are calculated to be $-80(-105)$ meV/% for the biaxial tensile strain and $-15(-60)$ meV/% for the uniaxial tensile strain, very close to the experimental data.

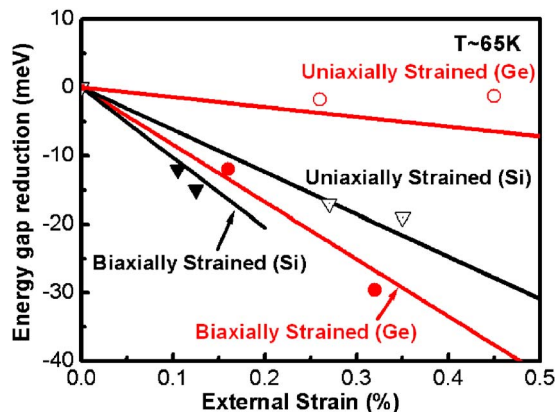


FIG. 5. Band gap reduction of strained Ge and Si due to strain. Biaxial strain gives more band gap reduction than uniaxial strain, and the reduction of Ge band gap is less than Si band gap under external strain.

In summary, we presented the EL spectra from the EHP recombination in the Ge MIS tunneling diode at different temperatures. The EL spectra can be fitted by a simple convolution of electron and hole distribution functions. The LA phonon and/or the band gap renormalization at high carrier density may be responsible for the reduction in Ge. With the external strain, the emission wavelength can be further turned.

This work is supported by the National Science Council of ROC under Contract Nos. 95-2221-E-002-370 and 95-2221-E-002-357.

- ¹H. Mimura, T. Matsumoto, and Y. Kanemitsu, *Appl. Phys. Lett.* **65**, 3350 (1994).
- ²Q. Mi, X. Xiao, J. C. Sturm, L. C. Lenchyshyn, and M. L. W. Thewalt, *Appl. Phys. Lett.* **60**, 3177 (1992).
- ³H. Presting, T. Zinke, A. Splett, H. Kibbel, and M. Jaros, *Appl. Phys. Lett.* **69**, 2376 (1996).
- ⁴W. Eisefeld, U. Werling, and W. Prettl, *Appl. Phys. Lett.* **42**, 276 (1983).
- ⁵C. W. Liu, M. H. Lee, M.-J. Chen, I. C. Chen, and C.-F. Lin, *Appl. Phys. Lett.* **76**, 1516 (2000).
- ⁶M. H. Liao, C.-Y. Yu, T.-H. Guo, C.-H. Lin, S. T. Chang, C.-T. Chai, and C. W. Liu, *IEEE Electron Device Lett.* **27**, 252 (2006).
- ⁷M. H. Liao, C.-Y. Yu, C.-F. Huang, C.-H. Lin, C.-J. Lee, M.-H. Yu, S. T. Chang, C.-Y. Liang, C.-Y. Lee, T.-H. Guo, C.-C. Chang, and C. W. Liu, *Tech. Dig. - Int. Electron Devices Meet.* **2005**, 1023.
- ⁸Y.-H. Kuo, Y. K. Lee, Y. Ge, S. Ren, J. E. Roth, T. I. Kamins, D. A. B. Miller, and J. S. Harris, *Nature (London)* **437**, 1334 (2005).
- ⁹P.-S. Kuo, B.-C. Hsu, P.-W. Chen, P. S. Chen, and C. W. Liu, *Electrochem. Solid-State Lett.* **7**, G201 (2004).
- ¹⁰M. H. Liao, M.-J. Chen, T. C. Chen, P.-L. Wang, and C. W. Liu, *Appl. Phys. Lett.* **86**, 223502 (2005).
- ¹¹M. H. Liao, P.-S. Kuo, S.-R. Jan, S. T. Chang, and C. W. Liu, *Appl. Phys. Lett.* **88**, 143509 (2006).
- ¹²B.-C. Hsu, W. T. Liu, C.-H. Lin, and C. W. Liu, *IEEE Trans. Electron Devices* **48**, 1747 (2001).
- ¹³<http://www.ioffe.rssi.ru/SVA/NSM/Semicond/>
- ¹⁴S. M. Sze, *Physics of Semiconductor Devices*, 2nd ed. (Wiley, New York, 1981), p. 15.
- ¹⁵C. W. Liu, M.-J. Chen, I. C. Chen, M. H. Lee, and C.-F. Lin, *Appl. Phys. Lett.* **77**, 1111 (2000).
- ¹⁶J. Weber and M. I. Alonso, *Phys. Rev. B* **40**, 5683 (1989).
- ¹⁷D. A. Kleinman, *Phys. Rev. B* **33**, 2540 (1986).
- ¹⁸X. Xiao, C. W. Liu, J. C. Sturm, L. C. Lenchyshyn, and M. L. W. Thewalt, *Appl. Phys. Lett.* **60**, 1720 (1992).
- ¹⁹*Properties of Crystalline Silicon*, EMIS Datareviews Series No. 20, edited by R. Hull (INSPEC, London, 1999), p. 404.
- ²⁰C. G. Van der Walle, *Phys. Rev. B* **39**, 1871 (1989).